Building and Environment 87 (2015) 82–91

Contents lists available at ScienceDirect

Building and Environment

journal homepage: www.elsevier.com/locate/buildenv

Accumulated snow layer influence on the heat transfer process through green roof assemblies

Mingjie Zhao [a], Jelena Srebric [b, *], Robert D. Berghage [c], Kevin A. Dressler [d]

[a] Department of Architectural Engineering, Pennsylvania State University, University Park, PA 16802, USA
[b] Department of Mechanical Engineering, University of Maryland, College Park, MD 20742, USA
[c] Department of Horticulture, Pennsylvania State University, University Park, PA 16802, USA
[d] Strategic Interdisciplinary Research Office, Pennsylvania State University, University Park, PA 16802, USA

ARTICLE INFO

Article history:
Received 23 August 2014
Received in revised form
22 December 2014
Accepted 23 December 2014
Available online 31 December 2014

Keywords:
Green roof
Snow
Heat transfer
Snow conductivity

ABSTRACT

A green roof can reduce the peak thermal cooling loads and reduce the building energy consumption during the summer. It is also necessary to understand the thermal performance of these green roof assemblies during the winter when affected by an accumulation of snow on the rooftops. This study presents an experimental investigation and discusses the snow influence on the heat transfer processes through green roof assemblies. The on-site experiments were conducted in the outdoor test facility in Pennsylvania, U.S.A. during the winter of 2010/2011. The experiments were conducted on green roof buildings and on reference buildings for comparison. The collected data included the local meteorology, building operation data, and manually measured snow properties. The measured heat fluxes show that the heat flow though the green roof assemblies compared to the typical roof assemblies were reduced by approximately 23% when there was not an accumulated snow layer. However, this difference in the heat flux was only 5% when the roof structure had an accumulated snow layer. To quantify the snow effects on the heat transfer through green roof assemblies, the Johansen method was then used for snow conductivity calculations on rooftops. These equations should be a part of the total energy balance for the snow covered green roof assemblies because the snow layer significantly altered the heat transfer through these roof assemblies.

1. Introduction

Green roof assemblies reduce the building's energy consumption by reducing the thermal loads through the building's roof in summer cooling conditions. Green roof assemblies also affect the building's energy load calculations when compared to the traditional roof assemblies. Specifically, green roof assemblies include additional roofing layers: (1) drainage layer, (2) substrate layer (growing media), and (3) vegetation layer. A number of previous studies performed experiments with green roof assemblies under summer conditions, and proved the ability of green roof assemblies to reduce the cooling loads utilizing experimental and numerical methodologies [1–5]. However, a few studies explored the influence of green roof assemblies on the building's heating loads as well as the influence of an accumulated snow layer on the heat transfer through the roof assembly. A study evaluated the green roof performance under mild winter conditions, and concluded that the influence of green roof assemblies is unimportant when focusing specifically on the heating loads [6]. However, the thermal performance of green roof assemblies may vary for different climate zones [5], so the results from regions with mild winters may not properly represent regions with cold winters. Another study, conducted in a cold climate, measured the thermal performance of a green roof versus a gravel roof. This study found that the temperatures of the insulation top layer and the roof membrane top layer were nearly identical for the two types of roof assemblies [7]. Another study confirmed that snow eliminates the potential heating energy savings by installing green roof assemblies, but the total energy savings were proved to be statistically significant regardless of the accumulated snow [8]. Additionally, an experimental study indicated that the snow layer has a strong influence on the heat transfer through the roof assembly, and reported that, with an accumulated snow layer, the green roof and the reference roof had

* Corresponding author. Tel.: +1 301 405 7276.
E-mail addresses: mxz190@psu.edu (M. Zhao), jsrebric@umd.edu (J. Srebric), rdberghage@mac.com (R.D. Berghage), kxd13@psu.edu (K.A. Dressler).

http://dx.doi.org/10.1016/j.buildenv.2014.12.018
0360-1323/

Nomenclature

K_{snow}	snow conductivity, W/(m·K)
K_{sat}	thermal conductivity of saturated snow, W/(m·K)
K_{dry}	thermal conductivity of dry snow, W/(m·K)
Ke	Kersten number, dimensionless
θ_{sat}	degree of saturation of the pores, dimensionless
ΔT	temperature difference of snow surface and bottom layer, °C
T_s	snow surface temperature, °C
T_b	snow bottom temperature, °C
T_a	temperatures of the air, °C
$T_{snowpack}$	temperature of the snowpack, °C
K_{ice}	ice conductivity, constant, 2.2 W/(m·K)
K_{air}	air conductivity at $T_{snowpack,}$ W/(m·K)
K_{water}	water conductivity at 0 °C, constant, 0.5475 W/(m·K)
ρ_{snow}	snow density, g/cm^3
ρ_{ice}	ice density, constant, 0.9167 g/cm^3
c	constant, when $T_{snowpack} < 0$ °C, c = 0.15, when $T_{snowpack} = 0$ °C, c = 0.3
V_{pores}	relevant fractions for bulk volume of pores in the snow dimensionless
V_{water}	relevant fractions for bulk volume of water in the snow, %
Q_{snow}	heat flux through the snow layer, W/m^2
$Q_{long\text{-}wave}$	downward long-wave radiation, W/m^2, measured from SURFRAD station
Q_e	flux of the latent heat (evaporation, sublimation, condensation) at the snow/air interface, W/m^2
Q_p	flux of heat from rain, W/m^2
Q_r	heat flux through the roof, W/m^2
Q_m	energy flux available for melt, kJ/(m^2·s)
Q_{sn}	net short-wave radiation flux absorbed by the snow, W/m^2
Q_{si} Q_r	incident and reflected radiation on the snow surface, W/m^2
Q_{ln}	net long-wave radiation flux at the snow/air interface, W/m^2
Q_{li}	the downward long-wave radiation at the snow-air surface, W/m^2
Q_{le}	upward radiation emitted by the snow surface, W/m^2
Q_h	convective or sensible heat flux from the air at the snow/air interface, W/m^2
D_h	bulk transfer coefficient for sensible heat transfer, kJ/(m^3·°C), liter
D_e	bulk transfer coefficient for latent heat transfer, kJ/(m^3·mbar), liter
U_Z	wind speed at the reference height, z is taken between 1 and 2 m, m/s
l	average snow depth, m
Δl	decrease of snow depth per day, m/d
h_f	latent heat of fusion, constant, 333.5 kJ/kg
B	thermal quality or the fraction of ice in a unit mass of wet snow, %
e_{air}, e_s	vapor pressures of the air and the snow surfaces, respectively, kPa
A	snow albedo, dimensionless
α	constant related to the inverse of the air-entry pressure, cm^{-1}
$q_{j,\theta}$	heat flux for time θ, W/m^2
$T_{s,abs}$	absolute temperature of the snow surface, K
ε_s	emissivity of snow, constant,0.97
σ	Stefan–Boltzmann constant, 5.64 × 10^{-8} W/m^{2}K^4

relatively the same seasonal heat losses [9]. However, the existing studies did not provide a calculation method to estimate the effect of snow on the heat transfer process through green roof assemblies. Therefore, for a better understanding of the thermal performance of green roof assemblies during the winter, the current study aims to experimentally validate a set of equations to account for the snow effect on the heat transfer through the green roof assemblies located in cold regions.

2. Experiment description

This study performed the on-site experiments in an outdoor test facility located in central Pennsylvania, USA. The data collection equipment was installed during the summer and fall of 2010. After the adjustment and calibration of the equipment, the data collection process lasted from the end of November 2010 until the end of February 2011. The data collection recorded two types of data: (1) heat flux, temperature and weather data continuously collected by the data acquisition system, and (2) snow properties discretely collected by manual measurements.

2.1. Layout of experimental site

The experimental site is located at the Russell E. Arson Research Center of the Pennsylvania State University near Rock Springs, PA, which is 24 km south from State College, PA, U.S.A. There are six identical buildings with a footprint area of 4.65 m^2 and a volume of 1.8 m × 2.6 m × 2.6 m. The buildings are spaced 6 m from each other and arranged in a 2 × 3 grid to ensure independent indoor and outdoor environments for all of the buildings. Specifically, the arrangement reduces the mutual blocking of wind, rain, and snow by the buildings, and allows for consistent exposure to the sun and weather elements. Among the six buildings, three of them have green roof assemblies with both a vegetation layer and a substrate layer. One building has a bare soil roof assembly with only a substrate layer and no vegetation layer on the rooftop. Finally, two buildings are reference roof buildings with neither a substrate layer nor a vegetation layer on the top of the original roof assemblies. All six buildings were constructed identically with the same wall assemblies, and the same locations of doors and windows. All roofs have a light slope (1/12) to maximize the solar exposure. Fig. 1 shows an overview of the experimental site with the building arrangement.

All of the six buildings have the same insulation layers with identical heating devices and air conditioning systems. A 1 kW thermostat controlled heating device is located at the south wall, and a 3 kW air conditioning system is installed in the north wall window of each building. The wall materials, from inside to outside, are 6.35 mm plywood, 89 mm fiber glass batting insulation with a thermal resistance (R-value) of 2.3 (m^2·K)/W and 6.35 mm oriented strand board (OSB) sheets. The materials of the reference roofs with the order from the inside to the outside are 6.35 mm OSB sheets, 89 mm fiber glass batting insulation, 19.05 mm plywood, and water proofing layer.

2.2. Green roof materials

The components of the green roof assemblies were identical for each building with a green roof. Beyond the roofing layers that the

Fig. 1. The outdoor test facility including buildings with and without the green roof assemblies.

reference buildings contain, the green roof buildings had additional layers from the bottom to the top including a plastic layer for roof protection, a drainage layer including a fabric layer, a substrate layer and a vegetation layer. The bare soil roof had the same layers, except the vegetation layer. Both the green roof and bare soil roof assemblies had a treated lumber framework around the edge of the substrate layer to protect and contain the substrate. The depth of the substrate layer was roughly 90 mm. The vegetation on the top of the green roof assemblies was *Sedum spurium*, which is commonly used for extensive green roofs. *Sedums* are hardy, succulent plants and have the ability to survive in drought and harsh conditions by limiting their water loss due to transpiration. The height of the vegetation layer ranged from 13 mm to 19 mm. The substrate was a mix of sphagnum peat moss, coir (coconut fiber), perlite, and hydrolite.

2.3. Data acquisition system and experimental procedures

In addition to the six small buildings, the experimental site had another control building that was equipped with a control computer which recorded data from the data acquisition system. The experiments included data collected by both installed data collection equipment and manual measurements. The data collection equipment continuously gathered data from a weather station for local meteorology data, and a sensor system for building operation data. The manual measurements took place during days with snow cover to collect snow properties.

2.3.1. Local meteorology data

The local meteorological data represented the outdoor environment for the experimental site. A weather station (WatchDog, 900 series) installed on the control building rooftop collected local meteorological data, including relative humidity (%), rain fall (ft), solar radiation (W/m^2), temperature (F), wind direction (Deg), wind gust (mph), and wind speed (mph). The data were collected every 30 s and averaged every 15 min.

2.3.2. Sensor system for measurement of building operation

A sensor system was established to measure the building operation parameters including temperatures of different roof layers (°C), snow depth (m), and heat flux through the roofs (W/m^2). Seven thermocouples measured roof assembly temperatures from roof bottom to top at the following locations: RI (roof inside), RO (roof outside), RD (roof drainage layer), RP (middle of soil layer), RS (roof surface), RM (plants temperature measured 2.5 cm above the substrate layer), and RT (air temperature measured 15.2 cm above the substrate layer). The reference buildings had three thermocouples that measured temperatures at RO (right above the insulation layer), RI (below the insulation layer), and RS (roof surface). Fig. 2 show the vertical locations of thermocouples for the two types of roof assemblies.

In addition to thermocouples, a heat flux meter (OMEGA, HFS-3) with the dimensions of 114.3 mm × 114.3 mm × 3.2 mm was adhered to the middle of the ceiling inside of each building. The sensors were calibrated to have a positive heat flux value which indicated heat transferred from the outside environment into the buildings. The collected data for heat fluxes were averaged every 15 min. Snow sonar depth sensors (MaxBotix, MB7070) were installed above the rooftops to collect averaged snow depth every 60 s, and to provide reference data for the manually collected measurements. Each building had a multiplexer (AM 16/32 Relay

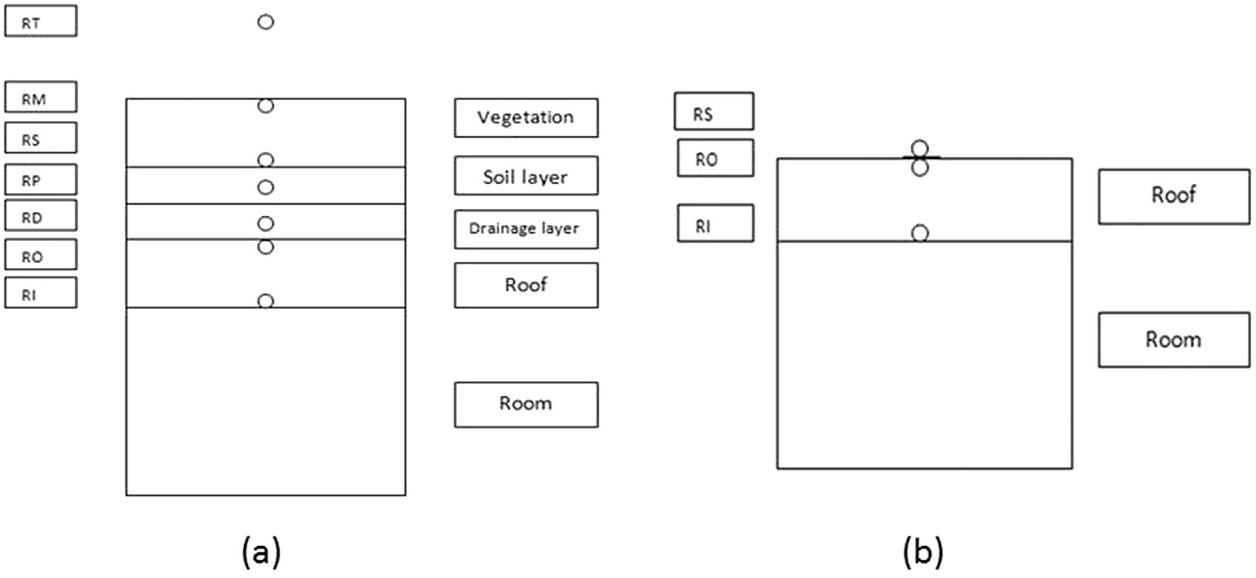

Fig. 2. Vertical locations of thermocouples for (a) green roof, and (b) reference roof assemblies.

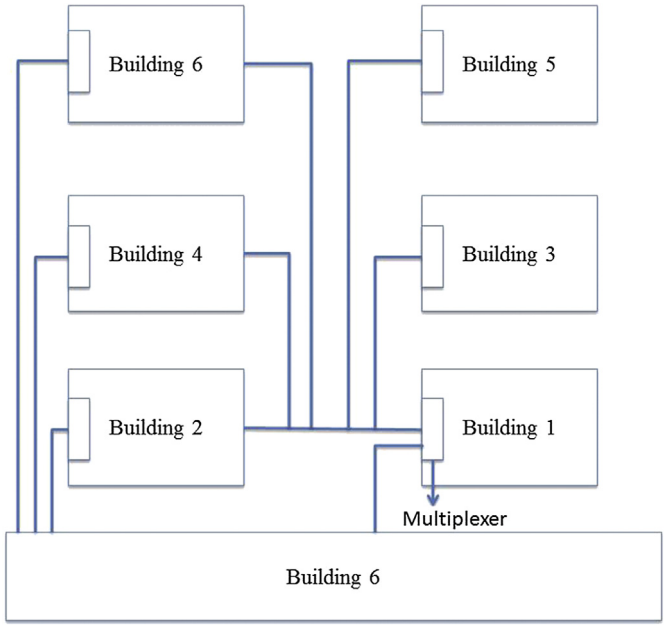

Fig. 3. Plan view of building layout and data acquisition system.

Multiplexer, Campbell Sci, Inc.) to collect the measured temperatures. An additional multiplexer was used to receive and transfer data signals from each building to two dataloggers (Campbell Sci, Inc, 23×). The dataloggers in the control building received all the signals from the multiplexers and sent the signals to the control computer. The computer then downloaded data from the dataloggers, and outputted and stored the data on a local hard drive. Fig. 3 shows the multiplexer and sensor connections for the buildings.

2.3.3. Manual measurements of snow properties

In addition to the automatic data acquisition system, manual data collection took place in a series of experiments to obtain discrete values of the snow properties. During this experimental period in January 2011, there were 11 days with manual measurements of snow properties. The manual measurements were conducted once a day, mostly around 10:00 AM in the morning. The manual measurements were performed sequentially for all 6 buildings, and the whole measurement process took approximately 2 h. A snow depth probe (Snowmetrics) was used to measure the average snow depth from five representative locations on the roofs, including one sample at the center of the roof and four samples roughly 20 cm from the snow edge. Snow board sampling equipment and a snow breeder (Snowmetrics) was used to measure the Snow Water Equivalence (SWE) and the heat flux through the snow layer. In addition, estimation of the liquid Water Content (mWC) and a range of liquid water content (θ) were determined with snow data available in the literature and presented in Table 1 [10].

3. Assumptions and methodology

The data analysis includes two steps: (1) quantification of the snow effect on the thermal performance of green roof assemblies by comparison with the thermal performance of the reference roofs, and (2) calculation of the snow conductivity to quantify the snow effect on the heat transfer process through the roofing assemblies. In the first analysis step, results showed that the accumulated snow layer eliminated the difference between the roofs thermal performance. In the second analysis step, a set of equations was validated from the measured data based on an existing calculation method for porous materials.

3.1. Snow layer assumptions

The study evaluates the snow effect on thermal performance of green roof assemblies by considering the accumulated snow as a layer of the roof assembly. A few assumptions have been made in order to investigate the heat transfer process through the snow covered roof assemblies:

1) The heat conduction was the major heat transfer mechanism considered inside the snow layer [11]. Therefore, the effective snow conductivity is the most important parameter to evaluate when analyzing the heat transfer process through the snow.
2) The heat flux through the roof assembly was assumed to be a one-dimensional and quasi-steady-state process that neglected the heat storage inside the substrate and snow layer. The temperature profile of the roof layers was linear and the temperature gradient was constant in terms of depth. This assumption simplifies the conductive heat transfer equation to become a linear equation, and helps account for the effect of snow conductivity.
3) The snow layer was a homogenous bulk layer, with well-distributed air and water inside the layer, and was considered a porous layer with negligible phase-change and impurity effects. The size of the ice grains was not considered, thus the snow can be seen as a homogenous layer in order to neglect mutual effects between snow grains.
4) The presence of vegetation above the snow surface can complicate the convective and latent heat exchanges, thus the vegetation layer was assumed to be buried by the snow with two reasons: (a) to ignore the vegetation effects on the snow conduction calculation [12] and (b) to assume well-defined, one-dimensional profiles of wind, temperature and humidity above the snow surface.
5) The snow surface temperature was assumed to equal the dew point temperature of the snow surface to simplify the complex measurements and calculations of snow surface temperature.

Table 1
The qualitative estimation of liquid water content (mWC) and the approximate range of liquid water content (θ) [10].

Wetness content	Index (mWC)	Description	θ (vol.%)
Dry	1	$T_s \leq 0$ °C. Disaggregated snow grains have little tendency to adhere to each other when pressed together.	0
Moist	2	$T_s = 0$ °C. The water is not visible, even at 10× magnification. When lightly crushed, the snow has a tendency to stick together.	0–3
Wet	3	$T_s = 0$ °C. The water can be recognized at 10× magnification by its meniscus between adjacent snow grains, but water cannot be pressed out by moderately squeezing the snow	3–8
Very Wet	4	$T_s = 0$ °C. The water can be pressed out by moderately squeezing the snow in the hands, but an appreciable amount of air is confined within the pores	8–15
Soaked	5	$T_s = 0$ °C. The snow is soaked with water and contains a volume fraction of air from 20 to 40%	>15

These assumptions allowed the heat transfer equations to use linear expressions and to neglect radiative fluxes inside the snow layer. Also, the homogeneity of the snow layer enables the use of bulk layer properties. Overall, these assumptions allowed the heat transfer phenomena to be accounted for with a reduced degree of complexity as long as the snow layer properties are available from manual measurements, such as the one conducted in this study.

3.2. Thermal performance of green roof buildings compared to reference buildings

The measured heat flux data was used as an indicator to evaluate the thermal performance of the different roof assemblies. This is due to the heat loss from the roof assemblies in winter directly affecting the heating loads and building energy consumption. Table 2 compares the measured heat fluxes for the green roof assemblies and the heat fluxes for the reference roof assembly for two continuous weeks of data collection. Since the microclimate significantly affects the relative thermal benefits of green roofs in winter [13], it is necessary to account for the effect of microclimate at the experimental site. Therefore, a few criteria were used to examine snow effect by comparing the two weeks with the most similar microclimate environments during the winter: (1) for the snow week, the building roofs should be covered by snow for the whole week, (2) for the non-snow week, no snowfalls on either day and no accumulated snow on all the roofs in that week, and (3) both snow week and non-snow week should be a continuous 7-day period for comparison, and the average daily temperature should be as close as possible for the two weeks (mean temperatures for non-snow and snow weeks are −1.1 °C and −2.8 °C, respectively). Due to lack of accurate control of microclimate, the result differences in Table 2 for snow week and non-snow week may be partly due to the microclimatic parameters, including the incoming solar radiation (mean solar radiation for non-snow and snow weeks are 46 and 76 W/m^2, respectively). In addition, Feb. 21st was used as the initial date for the observation snow week because all the roofs were fully covered after a big snow event on that day. There were other sparse snow events during the observation week. The experimental setup did not have instruments to continuously monitor snow accumulation, but the daily manual measurements did not show any significant accumulation during the observation week. Therefore, this study assumed that the original snow event at the beginning of the week was the source of the snow coverage, while the other events were assumed to be negligible. In this table, the minus value of heat flux indicates the heat losses from inside of the building to the outdoor environment. Table 2 shows that the buildings with the green roof assemblies experienced lower heat losses through the roof compared to the reference roof losses, independent of the snow layer presence. To compare the thermal performance of different roof types in more details, a previous study performed ANOVA analysis. The results showed that the effect of roof type on heat loss is statistically significant (p-value < 0.05), and concluded that the green roof buildings performed better than the reference buildings due to reduced heat losses of 5%–23% as shown in Table 2 [8].

Table 2
Comparison of green roof thermal performance based on measured heat fluxes.

Observed week	Snow conditions	Measured mean heat flux (W/m^2)		Energy saved by green roof assemblies (%)
		Green roof assemblies	Reference roof assemblies	
12/31/2010–01/06/2011	No snow	−7.1 ± 9.7[a]	−9.2	22.9
02/21/2011–02/27/2011	With accumulated snow	−9.1 ± 4.7[a]	−9.6	5.2

[a] These are the standard deviations for data collected at the three buildings with green roof assemblies. The standard deviations are relatively large since the mean heat flux indicates an average from 672 transient heat flux values including a few extreme values. This is possible due to the fluctuation of ambient environment during the measurement week.

Although the energy savings for buildings with the green roof assemblies during the heating seasons were confirmed, Table 2 indicates that the accumulated snow layer diminished the differences in heat losses and reduced energy savings enabled by the green roof assemblies without the snow layer. Specifically, the additional snow layer reduced the differences in surface albedo and emissivity for green roof and reference roof assemblies, so different assemblies, when covered with snow, had similar rooftop surface temperatures that resulted in similar conductive heat fluxes. Therefore, it is important to quantify the snow effect on the conductive heat transfer by calculating the conductivity of the snow layer.

3.3. Effective snow conductivity calculations

The heat transfer process inside the snow includes both sensible heat conduction and latent heat transfer. The sensible heat conduction may be dominant, but with a few restrictions, as described by the previous study of Kaempfer [14]. Therefore, the current study indicates validity of the snow conductivity calculated as the effective heat conductivity (EHC) of snow that aggregates: (1) conductivity through the ice matrix and the pore space, (2) the latent heat release and gain by recrystallization, and (3) the convective heat exchange between ice and pore air. These processes would be computationally intense to separate.

Based on the findings that the snow may have significant effects on the heat transfer process through building roofs, it is important to calculate the effective thermal conductivity of snow accumulated on a roof structure. A number of previous studies provided various methods to calculate the dry snow conductivity. In this study, the Johansen method for conductivity calculation in porous media was used to validate the equation for the wet snow conductivity [14,15].

Snow can affect the heat transfer process through the roof assemblies by modulating the intensity of the heat conduction. Based on the comparison of the measured and the simulated heat conductivities, a study suggested that the heat conduction through a snow layer is a dominant conduction component, being approximately 80% of the overall heat flow [16]. The snow conductivity varies for different types of snow layer conditions from loose to compact, from wet to dry, and from fresh snow to accumulated snow. The thermal conductivity of snow ranges from less than 0.1 W/(m·K) for fresh, less dense snow to greater than 0.51 W/(m·K) for more dense, ripened snow [17]. The difficulty for a snow conductivity calculation is to seamlessly present the variations of snow conditions, such as from dry to wet, from loose to compact. Different procedures have been developed to measure and calculate the snow conductivity, including field and laboratory measurements as the most common data collection methodologies. Table 3 shows the assumptions made for snow conductivity calculations in six previous studies [18–23]. Four of the studies assumed dry snow conditions to simplify the complexity of snow conduction calculations. Therefore, to quantitatively estimate the snow effect on roof assembles, this study validated an equation set that can be used for both dry and wet snow.

Table 3
Comparison of assumptions for calculating snow conductivity in existing literature.

Assumptions	Dry snow	Snow temperature	Phase-change	Air conduction
[15] Kaempfer and Plapp, 2009	Yes	n/a	Yes	Yes
[16] Schneebeli and Sokratov, 2004	n/a	About −8 °C	n/a	n/a
[17] Arons and Colbeck, 1998	Yes	n/a	n/a	No
[18] Liu and Si, 2008	Yes	below 0 °C	Ignore phase change near the heater needle	Yes
[19] Usowicz et al., 2008	Yes	n/a	n/a	n/a
[20] Sturm et al., 2002	n/a	n/a	n/a	No

The Johansen method used in this study is an interpolation approach to estimating the soil conductivity (K_{soil}) based on the thermal conductivity of dry soil (K_{dry}) and saturated soil (K_{sat}) [14]. Since snow is a porous material similar to soil, a few studies have utilized other soil research methods for snow investigations, and this study assumed the equations for the K_{soil} calculation can be used to estimate the snow conductivity (K_{snow}) [14]:

$$K_{snow} = (K_{sat} - K_{dry})K_e + K_{dry} \quad (1)$$

where Ke is the Kersten number, a dimensionless function of porous material's saturation degree given by the following linear equation:

$$K_e = a + b\log\theta_{sat} \quad (2)$$

where a and b are constants, and θ_{sat} is the degree of saturation of the pores.

Equations (1) and (2) are the primary equations validated for the calculation of snow conductivity. The equation deployment requires finding proper values for coefficients a, and b from the on-site measured data. The calculation of the other parameters in Equations (1) and (2) are presented as followed. The snow conductivity can also be represented by the heat flux through the snow layer and a temperature difference:

$$K_{snow} = -Q_{snow}l/\Delta T \quad (3)$$

$$\Delta T = T_s - T_b \quad (4)$$

where Q_{snow} (W/m^2) is the heat flux through the snow layer, l (m) is the measured snow depth, ΔT (°C) is the temperature difference between the snow surface and snow bottom, T_s (°C) is the snow surface temperature, and T_b (°C) is the measured snow bottom temperature.

Dry snow, defined as the snow without liquid water, and its conductivity K_{dry} can be calculated based on the air and ice conductivities [14]:

$$K_{dry} = \frac{(cK_{ice} - K_{air})\rho_{snow} + K_{air}\,\rho_{ice}}{\rho_{ice} - (1-c)\rho_{snow}} \quad (5)$$

$$T_{snowpack} = (T_s + T_b)/2 \quad (6)$$

where K_{ice} is the ice conductivity, 2.2 W/(m·K). K_{air} (W/(m·K)) is the air conductivity at $T_{snowpack}$, $T_{snowpack}$ (°C) is the temperature of the snowpack that is equal to 0 °C when the calculated results by Equation (6) are greater than 0, ρ_{snow} (g/cm^3) is the snow density calculated with the measured snow water equivalent, ρ_{ice} is the ice density that equals to 0.9167 g/cm^3, c is a constant, and when $T_{snowpack} < 0$ °C, c = 0.15, when $T_{snowpack} = 0$ °C, c = 0.3.

Saturated snow indicated wet snow under saturated conditions, and its conductivity K_{sat} can be calculated using the following equation [14]:

$$K_{sat} = K_{ice}^{1-V_{pores}} K_{water}^{V_{pore}} \quad (7)$$

$$V_{pores} = 1 - \frac{\rho_{snow}}{\rho_{ice}} \quad (8)$$

where K_{water} is the water conductivity at 0 °C, equal to 0.5475 W/(m·K), and V_{pores} is the relevant fraction for bulk volume of pores in the snow.

Finally, θ_{sat} indicates the liquid water fraction inside the snow layer and describes how saturated with liquid water the snow is. It can be calculated with the following equation:

$$\theta_{sat} = V_{water}/V_{pores} \quad (9)$$

where V_{water} is the relevant fraction for the bulk volume of water in the snow that was determined by the manual measurements. All of these equations enable snow conductivity calculations that account for both wet and dry snow layers. This distinction is significant for the heat transfer process because the layers of wet snow act as conductors, due to the presence of water, while the dry snow layers act as insulators, due to the presence of air.

3.4. Calculations of the snow surface temperature

The snow conductivity calculation, represented by Equation (3), requires an input of the snow surface temperature. However, the snow's surface temperature varies with the energy received through the snow surface [24]. Measuring the snow's surface temperature was not practical for this on-site experiment, so an energy balance model was used to calculate this temperature. The energy balance model was adopted from the literature [11]. This model represents a heat balance of the snow's surface and energy conservation of the entire snow layer with an assumption of a linear temperature profile within the snow.

The energy balance model for the snow layer includes the radiative and turbulent energy exchanges at the snow-air interface and the snow-roof interface. To account for these two heat transfer processes, the energy balance model requires an input of the incoming solar radiation, wind velocities, air temperatures, and humidity levels. The incoming solar radiation data were obtained from the SURFRAD network at State College, Pennsylvania [25], while the other data were measured at the experimental site. The SURFRAD station is located on the grounds of the Pennsylvania State University's agricultural research farm, and is maintained by the Meteorology department.

The amount of energy available for melting snow is determined from the energy equation [11]:

$$Q_m = Q_{sn} + Q_{ln} + Q_h + Q_e + Q_p - Q_r \quad (10)$$

where Q_m (W/m^2) is the energy flux available for snow melt process, Q_{sn} (W/m^2) is the net short-wave radiation flux absorbed by the snow, Q_{ln} (W/m^2) is the net long-wave radiation flux at the snow/air interface, Q_h (W/m^2) is the convective or sensible heat flux from the air at the snow/air interface, Q_e (W/m^2) is the flux of the latent heat (evaporation, sublimation, condensation) at the snow/air interface, Q_p (W/m^2) is the flux of heat brought from rain fallen on the snow, the current study does not consider this variable since rain fall was not present during the experimental period. Q_r (W/m^2) is the measured heat flux through the roof.

The daily amount of melt produced by a given value of Q_m is calculated by the following equation [11]:

$$Q_m = \Delta l \rho_{snow} h_f B \tag{11}$$

where Δl is (m/d) the decrease of snow depth per day indicating that the average depth changes by the evaporation or melting of the snow layer which is obtained from daily manual measurements, h_f is the latent heat of fusion that equals to 333.5 kJ/kg, and B (%) is the thermal quality or the fraction of ice in a unit mass of wet snow.

The snow surface has the potential to reflect a large portion of the short-wave radiation incident on the snow's surface, depending on its albedo value. Snow albedo (A) is the ratio of the reflected radiation (Q_r) to the incident radiation on the snow surface (Q_{si}), expressed as a decimal fraction or a percentage. Therefore, the net short-wave radiation flux absorbed by the snow (Q_{sn}) is calculated as follows:

$$Q_{sn} = (1 - A)Q_{si} \tag{12}$$

The snow surface albedo was considered a constant for each day, and the relationship between the albedo and the snow age (days) was used to determine the albedo values from the chart provided by the U.S. Army Corps of Engineers [11]. Based on this chart, the albedo values that are applicable to the snow cover in this study ranged from 0.56 to 0.71.

The net long-wave radiation at the snow-air surface (Q_{ln}) has two components: the downward solar radiation (Q_{li}), and the upward radiation emitted by the snow surface (Q_{le}). Typically, a snow surface has an upward radiation component greater than the downward radiation component, resulting in the negative value for the net long-wave radiation flux at the snow-air surface. With the downward long-wave radiation data available, the downward radiation component is calculated as following:

$$Q_{li} = \sigma Q_{long-wave} \tag{13}$$

where σ is the Stefan–Boltzzman constant that equals to 5.67×10^{-8} $W/(m^2 \cdot K^4)$, and $Q_{long\text{-}wave}$ (W/m^2) is the downward long-wave radiation.

The long-wave radiation emitted by the snow surface was calculated with the assumption that the snow layer represented a near-perfect black body in the long-wave portion of the spectrum. Therefore, the following equation applies to this assumption:

$$Q_{le} = \varepsilon_s \sigma T_{s,abs}^4 \tag{14}$$

where $T_{s,abs}$ (K) is the absolute temperature of the snow surface, and ε_s is the snow emissivity that equals to 0.97.

For the buildings with the green roof assembly, the ground heat transfer represented the heat transfer through the bottom of the snow layer and the top of the soil layer. Previous studies reported that an accurate evaluation of the heat fluxes across the snow-soil interface depends on the soil moisture content, infiltration of melt water, vapor transfer, and the magnitude of solar radiation that penetrates through the snow layer [26]. The methods to measure the soil heat transfer reported in previous studies include burying heat flow plates beneath the soil [27], and measuring the soil temperature profile in conjunction with the soil heat capacity to simulate the net gain or loss of heat within the soil layer [28]. The current study obtained the value of the ground heat fluxes by the heat flux sensors installed at the soil surface and in the middle of the roof surface.

The turbulent flux exchanges are of secondary importance while the net radiation flux exchanges are the controlling component in snow melt processes [11]. The turbulent exchange processes include turbulent convection in the snow-air surface due to the wind or the conduction when the wind is weak and therefore has little effect. The turbulent exchange processes occur in the air over the snow surface with a height of 2 m or 3 m, and two simplified expressions are proposed in the literature to estimate the Q_h and Q_e as following [11]:

$$Q_h = D_h U_z (T_a - T_s) \tag{15}$$

$$Q_e = D_e U_z (e_{air} - e_s) \tag{16}$$

where D_h ($kJ/(m^3 \cdot {}^\circ C)$) is the bulk transfer coefficient for sensible heat transfer, D_e ($kJ/(m^3 \cdot mbar)$) is the bulk transfer coefficient for

Table 4
Measured parameters of snow layer.

Dates	Parameters	Buildings					
		1	2	3	4	5	6
2/13/2011	l (m)	0.016	0.030	0.015	0	0	0.012
	ρ_{snow} (g/cm^3)	282.61	400	370.97	N/A	N/A	196.43
	SWE	4.52	12.10	5.49	N/A	N/A	2.36
2/23/2011	l (m)	0.062	0.077	0.068	0.068	0.061	0.068
	ρ_{snow} (g/cm^3)	250.00	256.25	260.00	279.07	314.52	270.83
	SWE	15.50	19.73	17.68	19.09	19.12	18.42
2/24/2011	l (m)	0.044	0.056	0.053	0.041	0.049	0.059
	ρ_{snow} (g/cm^3)	448.28	321.43	369.05	416.67	453.70	321.43
	SWE	19.89	17.94	19.69	17.00	22.37	18.93
2/26/2011	l (m)	0.033	0.042	0.041	0.027	0.029	0.042
	ρ_{snow} (g/cm^3)	406.25	300.00	312.50	379.31	388.89	333.33
	SWE	13.33	12.50	12.78	10.06	11.43	14.11
2/27/2011	l (m)	0.012	0.018	0.019	0.013	0.007	0.016
	ρ_{snow} (g/cm^3)	350.00	280.00	283.33	350.00	340.91	250
	SWE	13.33	12.50	12.78	10.06	11.43	14.11

Table 5
Calculated parameters for snow layer.

Dates	Parameters	Buildings					
		1	2	3	4	5	6
2/13/2011	K_{snow} W/(m·K)	0.17	0.53	0.01	N/A	N/A	0
	V_{pores}	0.69	0.56	0.60	N/A	N/A	0.79
	K_{sat} W/(m·K)	0.84	1.01	0.96	N/A	N/A	0.74
	K_{dry} W/(m·K)	0.28	0.43	0.39	N/A	N/A	0.19
	Q_{snow} (W/m^2)	5.94	9.96	2.49	N/A	N/A	0.37
2/23/2011	K_{snow} W/(m·K)	0.03	0.14	0.10	0.04	0.08	0.04
	V_{pores}	0.73	0.72	0.72	0.70	0.66	0.70
	K_{sat} W/(m·K)	0.80	0.81	0.81	0.84	0.88	0.83
	K_{dry} W/(m·K)	0.14	0.14	0.15	0.16	0.18	0.15
	Q_{snow} (W/m^2)	3.39	8.25	9.3	2.68	11.6	4.26
2/24/2011	K_{snow} W/(m·K)	0.61	0.60	0.32	0.56	0.66	0.32
	V_{pores}	0.51	0.65	0.60	0.55	0.51	0.65
	K_{sat} W/(m·K)	1.08	0.89	0.96	1.03	1.09	0.89
	K_{dry} W/(m·K)	0.30	0.19	0.22	0.27	0.30	0.19
	Q_{snow} (W/m^2)	30.9	11.1	12.7	25.8	35.7	6.26
2/26/2011	K_{snow} W/(m·K)	7.33	0.22	0.12	0.39	0.17	0.08
	V_{pores}	0.56	0.67	0.66	0.59	0.58	0.64
	K_{sat} W/(m·K)	1.01	0.86	0.88	0.97	0.99	0.91
	K_{dry} W/(m·K)	0.44	0.3	0.32	0.4	0.42	0.34
	Q_{snow} (W/m^2)	2.24	1.12	1.95	3.97	7.65	3.1
2/27/2011	K_{snow} W/(m·K)	0.04	0.05	0.05	0.02	0.01	0.01
	V_{pores}	0.62	0.69	0.69	0.62	0.63	0.73
	K_{sat} W/(m·K)	0.93	0.84	0.84	0.93	0.92	0.80
	K_{dry} W/(m·K)	0.36	0.28	0.28	0.36	0.35	0.24
	Q_{snow} (W/m^2)	20.7	11.5	11.5	20.2	19.4	4.85

latent heat transfer, U_Z (m/s) is the wind speed at the reference height Z, assumed to be between 1 m and 2 m, T_a and T_s (°C) are the temperatures of the air and the snow surface, respectively. The air temperature data collected by the weather station was used in the energy balance calculations to represent the ambient air temperature that played a significant role in the snow melt process. In addition, e_{air} and e_s (mbar) are the vapor pressures of the air and the snow surfaces, respectively.

The turbulent fluxes were derived from the estimated temperature and vapor pressure gradients between the snow's surface and the air at the reference height. In addition, e_a and T_a were measured at the same height as the height measurement of U_Z, with the reference height above the snow surface being 1 m. This study used the value for the bulk transfer coefficients D_h and D_e as established by the U.S. Army Corps of Engineers (1956), with the measurement at a reference height of 1 m for U_z, e_a and T_a. This results in the value for $D_h = 5.74 \times 10^{-3}$ kJ/(m^3·°C) and $D_e = 10 \times 10^{-3}$ kJ/(m^3·mbar). The atmospheric vapor pressure at the reference height was calculated using the air temperature and relative humidity data collected by the weather station. The snow surface vapor pressure was assumed to be the saturation vapor pressure of the air at the snow surface temperature ($e_s = e_{sat}(T_s)$).

This study accounts for the downward heat fluxes as positive and upward heat fluxes as negative, so the heat balance model of the snow layer can be written as:

$$Q_{sn} + Q_{li} - Q_{le} + Q_h + Q_e - Q_{snow} = 0 \quad (17)$$

4. Results and discussion

The heat balance model and on-site measured data allowed for the calculations of snow layer properties, including K_e and logθ, which are required to solve the snow conductivity equations. Table 4 lists the measured values of snow depth, snow density, and SWE from the on-site experiments, these variables were used to calculate the other snow properties listed in Table 5. The N/A values in the table indicate that there was no accumulated snow on the rooftops because the snow has already melted by the time of manual measurements. Fig. 4 shows the fitted regression line for the Kersten number equation $K_e = a + b\log\theta$, which was obtained by equation fitting for the relationship between K_e and logθ. This equation did not include a single data point that represented an outlier with the K_e value of 12.061, the result of the logθ input equal to −1.269 that was unrealistically high and indicated a measurement error. Furthermore, Table 6 shows the 28 calculated values of the Kersten number based on the measured and calculated parameters in Tables 4 and 5

Fig. 4 shows that after deleting the outlier, the R^2 of the fitted equation reached a value of 37.3%. Therefore, the equation set for a calculation of the wet snow conductivity is closed as following:

$$K_{snow} = \left(K_{sat} - K_{dry}\right)K_e + K_{dry} \quad (18)$$

$$K_e = 1.14 + 1.07\log\theta_{sat} \quad (19)$$

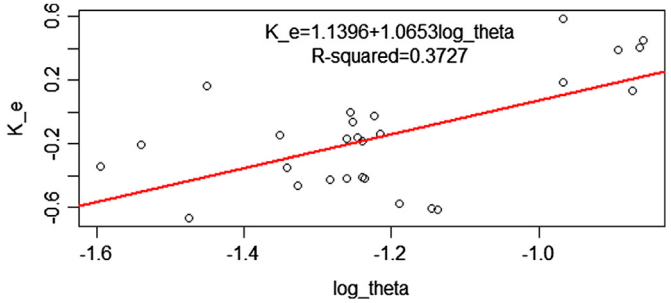

Fig. 4. Fitted line plot for the Kersten number K_e and saturation degree logθ. (The fitted linear relationship is highly dependent on the snow depth and the decrease of snow depth per day).

Table 6
Calculated values for the Kersten number K_e and the saturation degree logθ.

Date	2/13/2011		2/23/2011		2/24/2011		2/26/2011		2/27/2011	
Building	logθ	K_e	logθ	K_e	logθ	K_e	logθ	K_e	logθ	K_e
1	−1.539	−0.203	−1.260	−0.167	−0.863	0.402	−1.269	12.061	−1.189	−0.576
2	−1.450	0.166	−1.256	0	−0.967	0.586	−1.351	−0.142	−1.240	−0.409
3	−1.474	−0.664	−1.253	−0.063	−0.873	0.132	−1.342	−0.350	−1.237	−0.417
4	N/A	N/A	−1.240	−0.179	−0.892	0.389	−1.224	−0.024	−1.138	−0.612
5	N/A	N/A	−1.215	−0.141	−0.858	0.449	−1.283	−0.426	−1.145	−0.605
6	−1.594	−0.339	−1.246	−0.162	−0.967	0.185	−1.327	−0.461	−1.260	−0.419

Where:

$$K_{sat} = K_{ice}^{1-V_{pores}} K_{water}^{V_{pore}} \tag{20}$$

$$K_{dry} = \frac{(aK_{ice} - K_{air})\rho_{snow} + K_{air}\,\rho_{ice}}{\rho_{ice} - (1-a)\rho_{snow}} \tag{21}$$

$$V_{pores} = 1 - \frac{\rho_{snow}}{\rho_{ice}} \tag{22}$$

$$\theta_{sat} = V_{water}/V_{pores} \tag{23}$$

For a dry snow layer, θ_{sat} is equal to 0, so Equation (20) can be used to calculate the snow conductivity. For a wet snow layer, all of the six equations have to be used. With the assumptions made in this study, a few sources for bias may include:

(1) Assuming stable conditions and a linear temperature profile inside the snow layer may introduce a bias for sensible heat flux calculations due to the radiative heating above the snow surface which typically occurs during the snow melt process [29]. Furthermore, the single layer model could underestimate the sensible heat fluxes [30,31].
(2) The study simplified the calculation of turbulent flux in the energy balance model under the initial conditions. Under conditions of initial stability, the air layer above the snow surface can store evaporated water vapor from the snow, and subsequently this vapor can be heated by both direct and reflected solar radiation. As the air layer became warmer than either the snow surface or the ambient air above, it can re-radiate energy to the atmosphere and the snow. When the temperature of this air layer reaches the maximum, a sensible heat flux reversal may occur and result in an unstable condition. This phenomenon can also affect the water vapor flux calculation by the high vapor pressure maintained in the air layer [32].
(3) Another potential bias could be due to one of the major dilemmas in snow hydrology. The current study used an equation set to calculate the sensible and latent heat fluxes with the heat balance model on a routine, operational basis. However, the expressions of this equation set may not adequately describe the complicated interactions that can occur continuously in the snow/air interface [11]. In addition, the estimation of snow surface temperature was not from iteratively calculated heat fluxes of the snowpack, and the assumption of a linear snow temperature profile in the vertical direction may contribute to a overestimation of snow surface temperature [33].
(4) Assuming a constant bulk transfer coefficient could affect the accuracy of the latent heat transfer calculations. Since the melting snow layer has a rougher surface than that of smooth snow with the vegetation layer underneath, the bulk transfer coefficient for latent heat transfer can vary for the buildings with the green roof assembly during the experimental period [34].
(5) Neglected heat storage inside the snow and substrate, as well as dissipated heat through other directions during the heat transfer process, could result in an overestimation for the snow conductivity calculations.
(6) A few of the snow conductivity values obtained in the current study, and shown in Table 6, are relatively low. The reason is most likely due to the snow surface temperatures based on the existing empirical equations (Equations (11)–(16)). The snow surface temperature is directly proportional to the calculated conductivity because the indoor air temperature was constant during the experimental time period. The corresponding sensitivity analysis was performed by changing the snow surface temperature from −1 °C to 0 °C and found that the snow conductivity changed from 0.097 to 0.267, indicating that the accurate snow surface temperature is a critical parameter for the calculations of the snow conductivity. Since the microclimate affects the heat transfer through the roof assemblies by influencing the snow surface temperature [13], the assessment of this important parameter could affect the fidelity of the Johansen equations. Future studies should use both measured and calculated snow surface temperatures for the assessment of snow conductivity because simultaneous use of experimental and analytical methods can improve the fidelity of the snow surface temperature assessment.

The Johansen method was found to be useful for calculations of the soil conductivity based on the previous study, and this previous study also proposed that Johansen method is suitable for snow [14]. One of the major goals of the current study was to verify such statement because both snow and soil can be considered as porous media. The current study used the measured snow data and found the linear correlations for the coefficients in the Johansen equation that can be used for snow, which confirms the statement in the existing literature. Based on the measured parameters from the on-site experiments, the correlation between the Kersten number and the saturation degree was calculated for the coefficient of Johansen equation for snow. This correlation closed the system of equations required to solve the conductive heat transfer through a snow layer, depending on the snow wetness. Since the current study was based on extensive green roofs, the correlation coefficients are not be suitable for intensive green roofs, but the methodology of utilizing Johansen method for snow conductivity calculations may be used for other types of green roofs. In addition, the snow melting is a complicated process due to the changing snow properties, heat transferred inside the snowpack and between the snow, and the air and roof assemblies. Therefore, the assumptions made could limit the accuracy of this equation set. Nevertheless, this study

demonstrated that a snow layer significantly affected the roof heat losses, so the equation set is an efficient method to account for the snow effects on the roof heat transfer.

5. Conclusions

This study evaluated snow effects on buildings with green roofs by conducting on-site experiments in Pennsylvania, U.S.A. For the studied buildings during the time period without snow, the green roof assemblies reduced the building's heating energy consumption by 23% when compared to the energy consumption of the reference buildings with the traditional roof assemblies. However, this energy saving was reduced to 5% when a snow layer accumulated on the roofs. The possible reason for this significant reduction is that the additional snow layer on the rooftops affected the heat transfer process for both the green and reference roofs. Therefore, the current study validated an equation set to calculate snow conductivity and quantify the snow's effect on the heat transfer process on the roofs. The snow conductivity calculation depends on the water content in the snow layer. For the dry snow, this study used an equation based on the properties of ice, air, and snow. For the wet snow, the Johansen method for porous media was used as a linear function for a combined saturated and dry conductivity based on different Kersten numbers that represented varying saturation degrees. To validate the Johansen equation set for snow conductivity, a heat balance model of the snow layer was used to calculate the snow surface temperatures. With the on-site measured data, the linear relationship of the Kersten number and degree of snow pore saturation with a R^2 of 37.3% was developed. This allowed the effects of the snow on the heat transfer to be estimated by calculating the snow conductivity for the roof assemblies. Considering that the existing simulation programs do not calculate the heat transfer for the snow layer on green roofs, this model can support more accurate simulations of the heating loads and heating energy consumption for buildings with green roof assemblies.

Acknowledgments

This study was sponsored by the CMMI-0900486 award from the National Science Foundation (NSF), Division of Civil, Mechanical and Manufacturing Innovation (CMMI). Additional project results and sensitivity analyses are available at http://www.buildsci.us/modeling-of-natural-plant-materials.html.

References

[1] Sailor DJ. Thermal property measurements for ecoroof soils common in the western U.S. Energy Build 2008;40(7):1246–51.
[2] Tabares-Velasco PC, Zhao M, Peterson N, Srebric J, Berghage R. Validation of predictive heat and mass transfer green roof model with extensive green roof field data. Ecol Eng 2012;47(0):165–73.
[3] Tabares-Velasco PC, Srebric J. Predictive green roof model for assessment of heat transfer through a roof assembly in summer weather conditions. Build Environ 2012;49:310–23.
[4] Tabares-Velasco PC, Srebric J. A heat transfer model for assessment of plant based roofing systems in summer conditions. Build Environ 2012;49:310–23.
[5] Zhao M, Tabares-Velasco PC, Srebric J, Komarneni S, Berghage R. Effects of plant and substrate selection on thermal performance of green roofs during the summer. Build Environ 2014;78(0):199–211.
[6] Santamouris M, Pavlou C, Doukas P, Mihalakakou G, Synnefa A, Hatzibiros A, et al. Investigating and analysing the energy and environmental performance of an experimental green roof system installed in a nursery school building in Athens, Greece. Energy 2007;32(9):1781–8.
[7] Getter KL, Rowe B, Andresen JA, Wichman IS. Seasonal heat flux properties of an extensive green roof in a Midwestern U.S. climate. Energy Build 2011;43(12):3548–57.
[8] Zhao M, Srebric J. Assessment of green roof performance for sustainable buildings under winter weather conditions. J Central South Univ 2012;19(3):639–44.
[9] Liu K, Baskaran B. Thermal performance of green roofs through field evaluation. In: Proceedings for the first North American green roof infrastructure conference; 2003 [Chicago, IL].
[10] Techel F, Pielmeier C. Point observations of liquid water content in wet snow – investigating methodical, spatial and temporal aspects. Cryosphere 2011;5(2):405–18.
[11] Gray DM, Male DH. Handbook of snow: principles, processes, management & use. Toronto: New York Pergamon Press; 1981.
[12] Chung YC. Effects of vegetation and of heat and vapor fluxes from soil on snowpack evolution and radiobrightness. In: Geoscience and remote sensing symposium, 2006. IGARSS 2006. IEEE international conference on; 2006. p. 3746–9.
[13] Lundholm JT, Weddle BM, MacIvor JS. Snow depth and vegetation type affect green roof thermal performance in winter. Energy Build 2014;84(0):299–307.
[14] Balland V. Modeling soil thermal conductivities over a wide range of conditions. J Environ Eng Sci 2005;4(6):549–58.
[15] Andersland OB, Ladanyi B. An introduction to frozen ground engineering. New York: Chapman and Hall; 1994.
[16] Kaempfer TU. A microstructural approach to model heat transfer in snow. Geophys Res Lett 2005;32(21). 5-5.
[17] Zhang T. Influence of the seasonal snow cover on the ground thermal regime: an overview. Rev Geophys 2005;43(4). 23-23.
[18] Kaempfer TU, Plapp M. Phase-field modeling of dry snow metamorphism. Phys Rev E 2009;79(3):031502.
[19] Schneebeli M, Sokratov SA. Tomography of temperature gradient metamorphism of snow and associated changes in heat conductivity. Hydrol Process 2004;18(18):3655–65.
[20] Arons EM, Colbeck SC. Effective medium approximation for the conductivity of sensible heat in dry snow. Int J Heat Mass Transf 1998;41(17):2653–66.
[21] Liu G, Si BC. Dual-probe heat pulse method for snow density and thermal properties measurement. Geophys Res Lett 2008;35(16):L16404.
[22] Usowicz B, Lipiec J, Usowicz JB. Thermal conductivity in relation to porosity and hardness of terrestrial porous media. Planet Space Sci 2008;56(3–4):438–47.
[23] Sturm M, Perovich DK, Holmgren J. Thermal conductivity and heat transfer through the snow on the ice of the Beaufort Sea. J Geophys Res Oceans 2002;107(C10):8043.
[24] Kondo J, Yamazaki T. A prediction model for snowmelt, snow surface temperature and freezing depth using a heat balance method. J Appl Meteorol 1990;29(5):375–84.
[25] Commerce, U.S.D.o. and N.O.A. Administration, SURFRAD Network, Penn State, Pennsylvania; 2011.
[26] McKay DC. Measurements of the energy fluxes involved in the energy budget of a snow cover. J Appl Meteorol 1978;17(3):339–49.
[27] Monteith JL. The heat balance of soil beneath crops. Proc. symp. UNESCO arid zone res, vol. 11; 1958. p. 123–8.
[28] Slayter RO. Practical microclimatology. Australia: CSIRO; 1961.
[29] Leydecker A, Melack J. Evaporation from snow in the central Sierra Nevada of California. Nord Hydrol 1999;30(2):81–108.
[30] Halberstam I. Anomalous behavior of the atmospheric surface layer over a melting snowpack. J Appl Meteorol 1981;20(3):255–65.
[31] Males DH, Granger RJ. Energy and mass fluxes at the snow surface in a Prairie environment. 1979 [Hanover New Hampshire].
[32] Moore RD. On the use of bulk aerodynamic formulae over melting snow. Nord Hydrol 1983;14(4):193–206.
[33] Raj Singh P, Yew Gan T. Modelling snowpack surface temperature in the Canadian Prairies using simplified heat flow models. Hydrol Process 2005;19(18):3481–500.
[34] Gold LW, Williams GP. Energy balance during the snow melt period at an ottawa site. Div Build Res 1961;131:7.